

Energy absorption capacity of expanded metal meshes subjected to tensile loading

Capacidad de absorción de energía de mallas de metal expandido sometidas a tensión

Dimas José Smith-López¹, Carlos Alberto Graciano-Gallego^{2*}, Gennifer Nataly Aparicio-Carrillo³

¹Departamento de Mecánica y Tecnología de la Producción, Universidad Nacional Experimental Francisco de Miranda. Complejo Académico El Sabino, Prolongación Av. Táchira. C. P. 4102. Punto Fijo, Venezuela.

²Departamento de Ingeniería Civil, Facultad de Minas, Universidad Nacional de Colombia. Carrera 80 # 65-223 - Núcleo Robledo. A. A. 1027. Medellín, Colombia.

³Facultad de Ingeniería, Centro de Investigaciones en Mecánica (CIMEC), Universidad de Carabobo. Av. Universidad, Bárbula. C. P. 2005. Valencia, Venezuela.

ARTICLE INFO

Received November 25, 2014

Accepted May 27, 2015

KEYWORDS

Expanded metal, heat treatment, structural response, tensile force, energy absorption

Metal expandido, tratamiento térmico, respuesta estructural, fuerza de tracción, absorción de energía

ABSTRACT: Metallic energy absorption components should be able to absorb energy in different ways, depending on the type of the applied loads, namely axial compression, bending moment, shear loads, tensile forces, or a combination of these. A stable response through the whole deformation process is always expected, however, this depends essentially on geometrical parameters such as length and cross-section, as well as on material properties. Expanded metal meshes are manufactured upon an in-line expansion of partially slit metal sheets, creating a mesh with openings, formed by strands and bonds, a geometric configuration that may be exploited for energy-absorbing systems. This paper presents an experimental study on the structural response of expanded metal meshes (standard and flattened) subjected to tensile forces. The study also examines the influence of the annealing heat-treatment on the mechanical behavior of the expanded metal meshes. The results show that the flattened meshes are capable to absorb more energy than the standard ones. In addition, it is noticed that standard meshes are more sensitive in terms of the structural responses to the heat-treatments than the flattened meshes.

RESUMEN: Los componentes metálicos usados para absorber energía deben ser capaces de absorber la energía de diferentes maneras dependiendo del tipo de las cargas aplicadas, es decir, compresión axial, flexión, corte o fuerzas de tracción, o una combinación de éstas. Se espera siempre una respuesta estable a través de todo el proceso de deformación; sin embargo, esto depende esencialmente de parámetros geométricos como la longitud y la sección transversal, así como de las propiedades del material. Las mallas de metal expandido se fabrican mediante la expansión parcial en línea de láminas metálicas, creando una malla con aberturas formadas por venas y nodos, una configuración geométrica que puede ser aprovechada en sistemas que absorban energía. Este trabajo presenta un estudio experimental sobre la respuesta estructural de mallas de metal expandido (estándar y aplanadas) sometidas a fuerzas de tracción. El estudio también analiza la influencia del tratamiento térmico de recocido sobre el comportamiento mecánico de las mallas de metal expandido. Los resultados muestran que las mallas aplanadas son capaces de absorber más energía que los estándares. Además, se observa que las mallas estándares son más sensibles que las mallas aplanadas, en términos de la respuesta estructural a los tratamientos térmicos.

1. Introduction

After its invention, expanded metal has been widely used around the world for many years; as a consequence,

hundreds of patents are found in the literature regarding possible applications for expanded metal [1]. These applications fall into three main areas: furniture, construction, and energy-absorbing systems. In the manufacturing process of expanded metal sheets, the material undergoes slitting and stretching modifying the mechanical properties of the base metal, enhancing its strength. Additionally, there is a reduction of the weight per unit of area, which is an asset when designing lightweight structures. Expanded metal sheets are regularly fabricated [2] in two basic types: standard expanded metal (SEM) and flattened expanded metal (FEM). These two sheets are

* Corresponding author: Carlos Alberto Graciano Gallego

e-mail: cagracionog@unal.edu.co

ISSN 0120-6230

e-ISSN 2422-2844



quite different in geometry and mechanical properties. The flattened type undergoes additional cold-work, in which the standard sheet is passed through a cold-roll reducing mill. Figure 1 shows a typical expanded metal pattern.

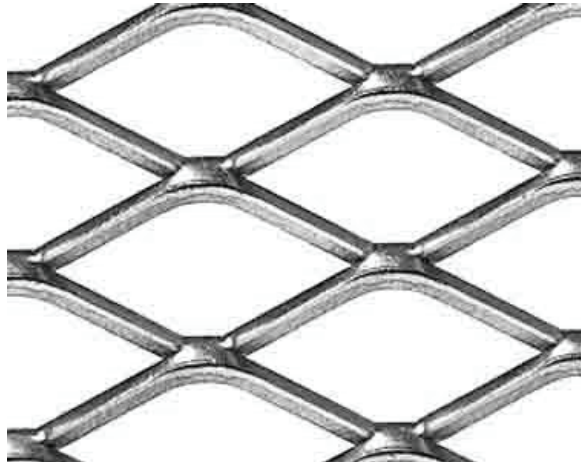


Figure 1 Typical standard expanded metal pattern

Currently, there is a search for new materials in engineering design; expanded metal is called upon giving an answer to several challenges. Waste material from the manufacturing process is almost none, since the base metal is cut and stretched to the final form. In addition, the use of expanded metal sheets reduces considerably the weight of any structural element or structure made of it.

Regarding energy absorption applications, metallic energy absorbers under axial compressive loads may fail in various modes, namely axial crushing, global and local buckling, depending essentially on geometrical parameters (length and cross-sectional variables). On the contrary, energy absorbers built on composite matrix fail due to a combined mechanism characterized by yielding and fracture. In [3], FEM sheets were used as core replacements for closed-cell honeycombs in sandwich panel structures. These pyramidal lattice trusses were tested under shear and through-thickness compression; the results showed improvements in collapse strength of these modified lattices. A series of experimental and numerical studies were conducted aimed at investigating the energy absorption capacity of SEM and FEM meshes used to absorb seismic energy in reinforced concrete moment resisting frames [4, 5]. In order to mitigate material damages under

hurricane conditions due to windborne debris impact from high-speed winds, [6] investigated a roofing system made of SEM panels, the results showed that the roofing system was able to resist penetration by heavy objects through the winds. A series of experimental and numerical studies have been conducted [7-9] on the collapse of tubes made of SEM meshes subjected to axial compression. The results showed that the collapse mechanism depends on the orientation of the expanded metal cells. The energy absorption capacity of the expanded metal meshes can be enhanced by either using FEM meshes [10] or adding material in concentric geometries [11].

The structural behaviour of SEM sheets under tensile loading was investigated numerically and experimentally [12]. The study was aimed at studying the influence of the expanded metal cell orientation with respect to the applied load. Thereafter, [13] conducted a series of experiments to obtain the mechanical properties of expanded metal sheets by correlating Vickers hardness measurements to yield strength values through Tabor relationship. It was found that the yield strength is higher in the nodes than in the strands of the expanded metal cells.

This paper is aimed at investigating the structural response of expanded metal meshes (SEM and FEM) subjected to tensile forces. The study also examines the influence of the annealing heat-treatment on the energy absorption capacity of expanded metal meshes.

2. Materials and methods

In this investigation, the expanded metal sheets were made from an ASTM A569 steel coil. Table 1 shows the chemical analysis of the base material determined experimentally using a spark emission spectrometer model SpectroLabIV. (a) HR, Hot Rolled; CQ, Commercial Quality

Figure 2 shows a schematic view of an expanded metal cell; the pattern is characterized by a rhomb shape with two orthogonal axes, a vertical one d_v in the slitting direction and a major one d_h . Besides, the pattern is composed of strands, with a thickness t and a width a , and connecting nodes that allow continuity in the mesh. Expanded metal meshes with two geometries, SEM and FEM, were studied in the experimental program; its characteristics are presented in Table 2.

Table 1 Chemical analysis of ASTM A569 steel, all elements in wt. %

| Specification | Description | Composition, % | | | | |
|---------------|-------------|----------------|--------|--------|--------|--------|
| | | C | Mn | P | S | Others |
| ASTM A569 | (a) HR-CQ | 0.0758 | 0.2295 | 0.0206 | 0.0072 | 0.0288 |

Table 2 Dimensions and technical specifications of the expanded metal meshes

| ASTM Designation | Code | Symbol | Catalog Name | Size mesh opening [mm] | | Strand [mm] | |
|------------------|---------|--------|---------------|------------------------|-------|-------------|------|
| | | | | dh | dv | t | a |
| A569-SEM | 0110791 | H-26 | 2" Mild steel | 89.60 | 44.20 | 3.00 | 3.20 |
| A569-FEM | 0110793 | H-26 | 2" Mild steel | 89.60 | 44.20 | 3.00 | 3.20 |

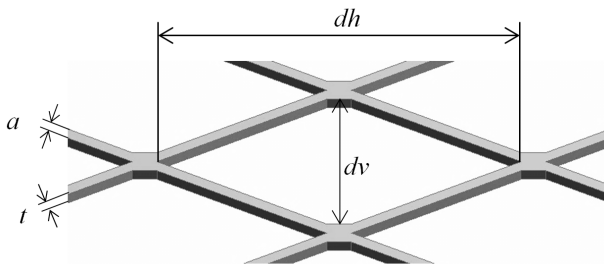


Figure 2 Schematic view of an expanded metal cell

It is important to point out that FEM meshes are the result of flattening SEM meshes; it indicates that to obtain the former, the mesh undergoes further plastic deformation when passed through the cold-rolling process, and the strands are also twisted, enhancing both the yield strength and the bending capacity of the strands for FEM meshes. Recently, [13] demonstrated empirically using Tabor's equation, that the yield strength for FEM meshes is greater than for SEM meshes.

In order to investigate the influence of the annealing on the energy absorption capacity of the meshes, a temperature of 950 °C and eight exposure times, ranging from 15 minutes to 120 minutes in 15 minutes steps, were selected. To guarantee repeatability [14], these variations of the heat-treatment were applied to three samples of each mesh type, SEM and FEM, totaling 48 annealed specimens; *i.e.* 24 SEM specimens and 24 FEM specimens. Additionally, six samples in as-received condition were used for reference. The purpose of applying annealing with different exposure times was to cause differences in the microstructure of the specimens. An Electric Resistance Furnace JH®, model HET. 80, was used for the heat treatments. The inside temperature of the furnace was controlled at every moment during the early stages of heating.

According to the ASTM Standard E 8M-04 [15], the specimens were subjected to tensile load using a Page Wilson servo-hydraulic testing machine model 60HD with a load cell of 20 Ton capacity. The axial load-displacement history was measured at a cross-head speed of 5 mm/min. A personal computer equipped with the PACAM-PA/MPC.2a v1.3 data acquisition software [16], was used to record the measurements from the load cell.

Figure 3 shows a schematic view of the tested specimens; the samples had width of 180.00 ± 1.54 mm, a full length of

420.00 ± 6.87mm and a free testing length of 270.00 ± 3.23 mm. At the end of the specimens, a steel plate of 190.00 ± 2.12 mm in width, 75 ± 1.14 mm in length, and 3.20 ± 0.12 mm thickness was welded in order to distribute uniformly the applied load by the machine loading platens, and to avoid excessive stress concentration on the mesh ends. Finally, the specimens were fixed to the equipment using a gripping device especially designed for this purpose as shown in Figure 3.

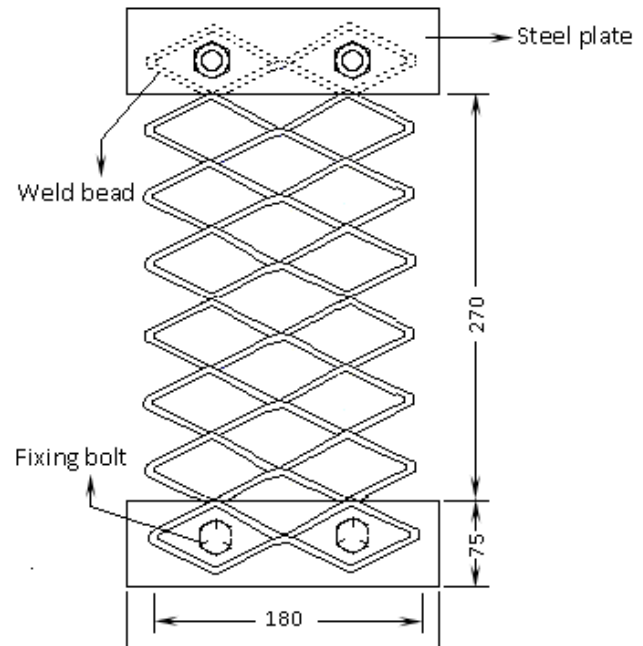


Figure 3 Geometry and dimensions in (mm) for the test specimens

3. Results and discussion

3.1. Load-displacement responses and deformation patterns

Figure 4 illustrates the progressive displacement observed in the SEM and FEM specimens tested under tension. This deformation sequence is consistent with the results obtained in [10].

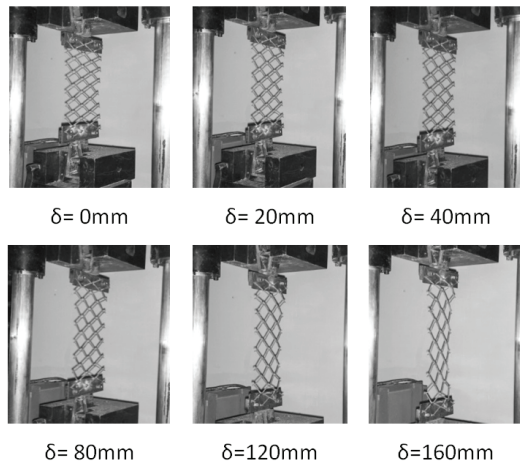


Figure 4 Progressive displacement of as-received condition SEM meshes under tensile loading

All tested samples underwent progressive collapse characterized mainly by bending of the strands in the areas close to the nodes. From a structural point of view, the peak load is achieved when the plastic capacity of the strands is attained, it means that plastic hinges are attained and the material yields freely, until the cells are closed.

Figures 5a and 5b show the average load-displacement curves of SEM and FEM specimens, respectively, in both, as-received and annealed conditions for the different stages of heating at 950 °C, with a exposure time ranging from $t=15$ min to $t=120$ min, at 15 min intervals. Regarding the structural behavior of the specimens, the responses are very stable for both specimens, exhibiting a gradual load increase until a plateau region is reached; i.e. the initial peak load F_{peak} is reached, and then the load remains almost constant with increasing displacements. This behavior

is desirable for energy-absorbing systems, where energy should be absorbed in a stable and controlled manner.

A significant scatter is observed in the responses as the exposure time changes for SEM specimens (Figure 5a). For FEM specimens the main variation occurred between the specimens in as-received condition and the remaining annealed specimens. In the latter, the energy absorption characteristics remained almost constant as observed in Figure 5b. A closer look at the load-displacement responses for SEM and FEM meshes, in as-received conditions, show a significant enhancement in the response for FEMs. As mentioned earlier, the yield strength and the cross-section of the strands are larger due to the flattening process.

3.2. Energy absorption properties

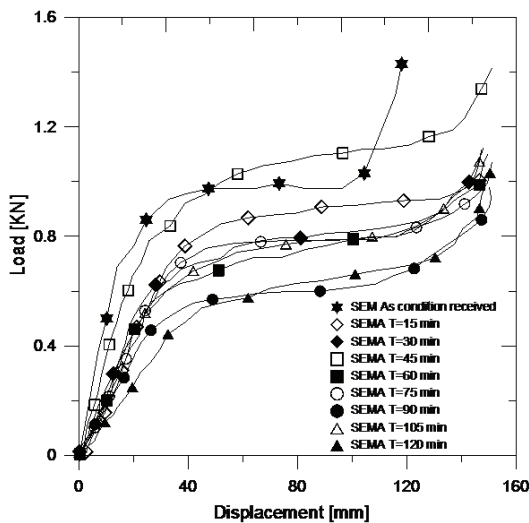
Tables 3 and 4 shows the experimental results (average) for the expanded metal meshes tested herein. The measured response parameters were initial peak load (F_{peak}), mean load (F_m), and the energy absorbed (E_a).

The energy absorbed E_a , is calculated with Eq. (1) by integrating the load-displacement curves as:

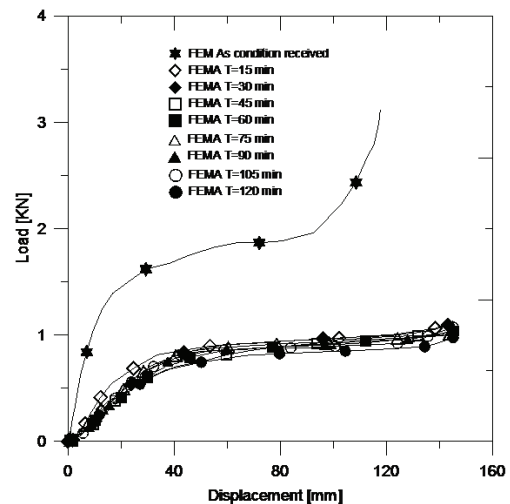
$$E_a = \int_0^d F(x) dx \tag{1}$$

where F is the tensile force, d and x are the stretching length and displacement, respectively. The mean force F_m is defined by Eq. (2):

$$F_m = \frac{E_a}{d} = \frac{1}{d} \int_0^d F(x) dx \tag{2}$$



(a) SEM specimens



(b) FEM specimens

Figure 5 Average load-displacement responses for SEM and FEM specimens in as-received and annealed conditions (from $t=15$ min to $t=120$ min at 950 °C)

Table 3 Average energy absorption characteristics for SEM meshes

| Time (min) | F_{peak} (kN) | F_m (kN) | E_a (J) |
|-----------------------|-----------------|------------|-------------|
| As-received condition | 0.88 ±0.03 | 0.89±0.03 | 106.21±3.45 |
| 15 | 0.80±0.12 | 0.77±0.03 | 115.50±4.52 |
| 30 | 0.70±0.09 | 0.72±0.02 | 108.14±3.21 |
| 45 | 0.94±0.04 | 0.96±0.02 | 144.26±7.41 |
| 60 | 0.64±0.03 | 0.68±0.03 | 101.94±3.56 |
| 75 | 0.73±0.11 | 0.70±0.05 | 104.74±1.85 |
| 90 | 0.55±0.18 | 0.56±0.08 | 84.14±4.95 |
| 105 | 0.66±0.02 | 0.70±0.01 | 104.84±5.66 |
| 120 | 0.54±0.09 | 0.55±0.04 | 82.86±1.83 |

Table 4 Average energy absorption characteristics for FEM meshes

| Time (min) | F_{peak} (kN) | F_m (kN) | E_a (J) |
|-----------------------|-----------------|------------|-------------|
| As-received condition | 1.50±0.02 | 1.73±0.03 | 207.65±5.95 |
| 15 | 0.84±0.01 | 0.84±0.02 | 122.43±2.56 |
| 30 | 0.80±0.02 | 0.81±0.01 | 117.54±4.98 |
| 45 | 0.71±0.02 | 0.76±0.02 | 110.56±1.94 |
| 60 | 0.81±0.02 | 0.77±0.03 | 111.06±3.56 |
| 75 | 0.78±0.01 | 0.77±0.01 | 112.36±0.98 |
| 90 | 0.80±0.03 | 0.79±0.02 | 115.31±1.33 |
| 105 | 0.81±0.01 | 0.77±0.02 | 111.73±1.72 |
| 120 | 0.69±0.03 | 0.71±0.01 | 103.04±1.36 |

The results presented in Tables 3 and 4 were calculated from the average load-displacement curves shown in Figure 5. These results show that the highest peak loads F_{peak} are obtained for the as-received condition specimens, 0.88kN and 1.50kN for SEM and FEM specimens, respectively. As discussed in the previous section, this enhancement for FEM meshes is ought to an increase in the yield strength and bending capacity, and hence the mechanical properties in the bonds strongly influence the tensile response.

The experimental results also reveal the variation in the energy absorption characteristics of the SEM and FEM meshes due to the annealing. For SEM specimens in Table 3 the peak load is reduced 38.6%, from $F_{peak}=0.88$ kN for the as-received specimens to 0.54kN for the specimens annealed 120min. This reducing trend is also observed for the mean load F_m . Nevertheless, the absorbed energy E_a increases and the response become smoother (Fig. 5a) for the annealed specimens, the largest increase is observed for the specimens with an exposure time of t=45min.

For FEM specimens, the energy absorption characteristics are considerably reduced after annealing, with slight changes in terms of the exposure times. In Table 4, it is observed that the peak load for the as-received specimen is $F_{peak}=1.50$ kN, and for the specimen exposed 120min is $F_{peak}=0.69$ kN, that represents a reduction of 64%. Comparing the remaining two parameters, mean load and energy absorbed, for these specimens similar results are attained. However, a comparison of the energy absorption characteristics for the annealed FEM specimens shows low variability in the corresponding values. As an example, for a specimen with exposure time t=15min: $F_{peak}=0.84$ kN, $F_m=0.84$ kN, and $E_a=122.43$ J; and for a specimen with a exposure time t=105min the corresponding values are $F_{peak}=0.81$ kN, $F_m=0.77$ kN, and $E_a=111.73$ J. From the results presented in Tables 3 and 4, it is possible to conclude that annealing induced relaxation of residual stress caused during the flattening process, and then causing a more uniform response and energy absorption characteristics for the FEM specimens.

4. Conclusions

The energy absorption capacity of expanded metal meshes (standard and flattened) subjected to tensile loading was investigated experimentally herein. This study also examined the influence of annealing with different exposure time on the mechanical behavior of the expanded metal meshes. From the experimental results, the following conclusions can be drawn:

- Annealing reduces the energy absorption capacity of expanded metal meshes subjected to tensile loading. This reduction in capacity increases with the exposure time for SEM meshes.
- The energy absorption characteristics can be substantially improved by flattening the SEM meshes, *i.e.* by using FEM meshes.

Furthermore, this paper represents a contribution to the understanding of the structural behaviour of expanded metal in energy absorption applications.

5. Acknowledgments

The authors gratefully acknowledge the support of the Laboratory of Material Sciences and the Technology Research Center (CITEC) of the Universidad Francisco de Miranda, Universidad de Carabobo, INCES-Falcón, and the Universidad Simón Bolívar for this study.

6. References

1. D. Smith, C. Graciano and G. Martínez, "Recent patents on expanded metal", *Recent Patents on Materials Science*, vol. 2, pp. 209-225, 2009.
2. National Association of Architectural Metal Manufacturers (NAAMM), *Standards for expanded metal*, Standard EMMA 557-12, 2012.
3. G. Kooistra and H. Wadley, "Lattice truss structures from expanded metal sheet", *Materials & Design*, vol. 5, no. 2, pp. 507-514, 2007.
4. P. Dung and A. Plumier, "Behaviour of expanded metal panels under shear loading", in *International Colloquium Stability and Ductility of Steel Structures* (SDSS'Rio), Rio de Janeiro, Brazil, 2010, pp. 1101-1108.
5. P. Dung, "Seismically retrofitting and upgrading RC-MRF by using expanded metal panels", Ph.D. dissertation, University of Liege, Liege, Belgium, 2011.
6. M. Rambo, P. Mtenga and K. Walsh, "Missile impact resistance of a metal mesh roofing system", *Journal of Architectural Engineering*, vol. 18, no. 3, pp. 199-205, 2012.
7. C. Graciano, G. Martínez and D. Smith, "Experimental investigation on the axial collapse of expanded metal tubes", *Thin-Walled Structures*, vol. 47, no. 8-9, pp. 953-961, 2009.
8. C. Graciano, G. Martínez and A. Gutiérrez, "Failure mechanism of expanded metal tubes under axial crushing", *Thin-Walled Structures*, vol. 51, pp. 20-24, 2012.
9. G. Martínez, C. Graciano and P. Teixeira, "Energy absorption of axially crushed expanded metal tubes", *Thin-Walled Structures*, vol. 71, pp. 134-146, 2013.
10. D. Smith, C. Graciano, G. Martínez and P. Teixeira, "Axial crushing of flattened expanded metal tubes", *Thin-Walled Structures*, vol. 85, pp. 42-49, 2014.
11. D. Smith, C. Graciano and G. Martínez, "Quasi-static axial compression of concentric expanded metal tubes", *Thin-Walled Structures*, vol. 84, pp. 170-176, 2014.
12. G. Martínez, C. Graciano, E. Casanova and O. Pelliccioni, "Estudio del comportamiento estructural de mallas de metal expandido sometidas a tracción", *Boletín Técnico IMME*, vol. 46, no. 2, pp. 37-52, 2008.
13. D. Smith, C. Graciano and G. Aparicio, "An empirical method for the estimation of yield strength on bonds and strands of expanded metal meshes", *Rev. Fac. Ing. Univ. Antioquia*, no. 74, pp. 132-142, 2015.
14. G. Box, J. Hunter and W. Hunter, *Statistics for experimenters: Design, Innovation and Discovery*, 2nd ed. New Jersey, USA: Wiley, 2005.
15. American Society for Testing and Materials (ASTM International), *Standard Test Methods for Tension Testing of Metallic Materials*, Standard ASTM E 8M-04, 2004.
16. Universidad Nacional Experimental Francisco de Miranda, *Manual de Funcionamiento de la Máquina Universal de Ensayos Mecánicos PAGE WILSON MEASUREMENT SYSTEMS MODELO 60HD SERIAL 826936*. Punto Fijo, Venezuela: CITEC-UNEFM, 2003.